2014 IEEE International Conference on Fuzzy Systems (FUZZ-IEEE)
July 6-11, 2014, Beijing, China

Analysis of the Performances of Type-1, Self-Tuning Type-1 and Interval Type-2 Fuzzy PID Controllers on the Magnetic Levitation System

Ahmet Sakalli, Tufan Kumbasar, Engin Yesil, and Hani Hagras

Abstract—**In this paper, we will compare the closed loop control performance of interval type-2 fuzzy PID controller with the type-1 fuzzy PID and conventional PID controllers counterparts for the Magnetic Levitation Plant. We will also compare the control performance of the interval type-2 fuzzy PID controller with the self-tuning type-1 fuzzy PID controllers. The internal structures of implemented controllers are firstly examined and then the design parameters of each controller are optimized for a given reference trajectory. The paper also show the effect of the extra degree of freedom provided by antecedent membership functions of interval type-2 fuzzy logic controller on the closed loop system performance. The real-time experiments are accomplished on an unstable nonlinear system, QUANSER Magnetic Levitation Plant, in order to show the superiority of the optimized interval type-2 fuzzy PID controller compared to optimized PID and type-1 counterparts.**

Keywords—Interval type-2 fuzzy PID controllers; self-tuning; magnetic levitation system.

I. INTRODUCTION

In the fuzzy control literature, ordinary (type-1) Fuzzy PID controllers (FPID) are often mentioned as an alternative to conventional PID controllers since they are analogous to the PID controllers from the input-output relationship point of view [1]-[3]. Numerous techniques have been developed in the literature for analyzing and designing a wide variety of Type-1 Fuzzy PID (T1-FPID) control systems [3]-[6]. The design parameters of the T1-FPID controllers can be summarized within two groups, structural parameters and tuning parameters [6]. The structural parameters include input/output variables to fuzzy inference such as fuzzy sets, Membership Functions (MFs) shapes, rules and inference mechanism. Tuning parameters include input/output Scaling Factors (SFs) and the parameters of the MFs. After the pioneering study by Qiao and Mizumoto [3], various online tuning mechanisms have been presented to improve the control performance of the fuzzy control system in presence of parameter variations and nonlinearities [7]-[10]. Thus, Self-Tuning Type-1 Fuzzy PID (STT1-FPID) controllers have been proposed where the SFs or the parameters of MFs have been adjusted in an online manner [7]-[12]. However, the main research focus was on the tuning of the SFs since their effect on the system response can easily be observed [8]-[9]. The presented self-tuning mechanisms for the SFs provide extra degrees of freedom to the fuzzy control structure, but also enhance new tuning structures which have to be determined (update functions or extra fuzzy inference mechanisms).

Recently, researchers began investigating Interval Type-2 Fuzzy Logic Controllers (IT2-FLCs) which have demonstrated significant control performance improvements in comparison to its type-1 counterpart [13]-[15]. It has been shown in various works that the T1-FPID controllers using Type-1 Fuzzy Sets (T1-FSs) might not be able to fully handle the high levels of uncertainties associated with control applications while the Interval Type-2 Fuzzy PID (IT2-FPID) controller using Interval Type-2 Fuzzy Sets (IT2-FSs) might be able to handle such uncertainties to produce a better control performance [15]-[17]. It has been shown in various works that IT2-FPIDs achieve better control performances because of the additional degree of freedom provided by the Footprint of Uncertainty (FOU) in their antecedent MFs [14]-[15],[18]. In literature, the design of the IT2-FPID controllers is usually solved by extending MFs of an existing T1-FPID controller or by employing optimization algorithms [19]-[21].

In this paper, we will present comparative real-time results between T1-FPID, STT1-FPID and IT2-FPID controller structures on the QUANSER Magnetic Levitation Plant (MAGLEV). We will also compare the results of IT2-FPID controller with two STT1-FPID controller structures which are based on the Function Tuner (FTT1-FPID) and based on the Relative Rate Observer (RROT1-FPID). The employed self-tuning mechanisms allow the T1-FPID structures to have more degrees of freedom. Thus, we will investigate if the power of the IT2-FPID lies in its ability to handle the high level of uncertainties rather than only having an extra degree of freedom. We will first present brief information about the internal structures of the employed FPID controller structures and then present their design strategies. We implemented the presented FPID controllers in a cascade structure to solve the control problem of the MAGLEV. A detailed comparative study has been conducted to show that the real-time control performance of the IT2-FPID is better in different operating points even at those at which the controllers are not optimized and IT2-FPID control system is more robust against noise and unknown system dynamics when compared to its T1-FPID, STT1-FPID and traditional PID counterparts.

A. Sakalli, T. Kumbasar and E. Yesil are with the Department of Control and Automation Engineering, Istanbul Technical University, Istanbul, Turkey (e-mail: {sakallia, kumbasart, yesileng}@itu.edu.tr)

H. Hagras is with the Computational Intelligence Centre, University of Essex, Colchester, United Kingdom (e-mail: hani@essex.ac.uk)

This research is supported by the Scientific and Technological Research Council of Turkey (TUBITAK) under the project (113E206). All of these supports are appreciated.

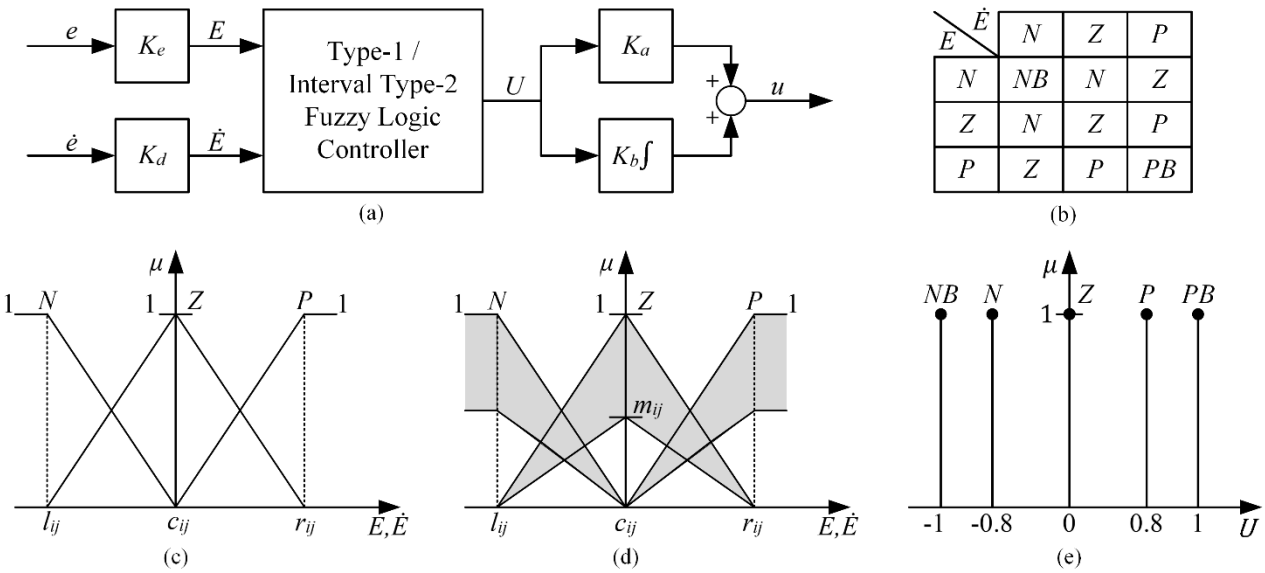

Fig. 1. Illustration of the (a) T1-FPID / IT2-FPID controller structure, (b) Rule base of T1-FLC and IT2-FLC, (c) Antecedent MFs of T1-FLC, (d) Antecedent MFs of IT2- FLC, (e) Consequent crisp singleton MFs of T1-FLC and IT2-FLC

Section II will briefly present the internal structures of the T1-FPID, STT1-FPID and IT2-FPID controller and design strategies, Section III will present cascade control system design strategy for MAGLEV and the real-time experimental results. Section IV will present conclusions.

II. Design Strategies of Type-1 and Interval Type-2 Fuzzy PID Controllers

In this section, we will present the structures and design strategies of the employed T1-FPID, STT1-FPID and IT2-FPID controllers. The FPID controllers are constructed by choosing the inputs to be error (e) and change of error ($\dot{e}$) and the output as the control signal (u) as shown in Fig.1a. Here, the input SFs K_e (for e) and K_d (for $\dot{e}$) normalize the inputs to the universe of discourse where the MFs of the inputs are defined. Thus e and $\dot{e}$ are converted after normalization into E and $\dot{E}$ while the output (U) of the T1-FLC/IT2-FLC is converted into the control signal (u) by the output SFs K_a (proportional SF) and K_b (integral SF) [9].

A. Design Strategies of the Type-1 Fuzzy PID Controllers

In this subsection, we will present the structure and the design strategies of the employed T1-FPID controllers. In the handled T1-FPID structure, a symmetrical 3x3 rule base is used as shown in Fig.1b. The rule structure is as follows:

$$R_q\text{: If } E \text{ is } A_{1j} \text{ and } \dot{E} \text{ is } A_{2j} \text{ THEN } U \text{ is } C_q, \quad i,j = 1,2,3;\ \ q = 1,\dots,Q = 9 \tag{1}$$

where A_{1j} is and A_{2j} are the antecedent MFs for the inputs E and $\dot{E}$, respectively, C_q is the consequent crisp set and Q is the number of rules.

In this study, we will employ three T1-FSs for each input domain (E and $\dot{E}$) and denote them as *N* (Negative), *Z* (Zero) and *P* (Positive). The T1-FSs of the T1-FLC are defined with three parameters (l_{ij}, c_{ij}, r_{ij}; *i=1,2, j=1,2,3*), as shown in Fig.1c and are set as l_{11}=l_{21}=-1, c_{11}=c_{21}=0, r_{11}=r_{21}=1. The consequent part is defined with five singleton consequents, as shown in Fig.1e, which are Negative Big (*NB*) = -1, Negative (*N*) = -0.8, Zero (*Z*) = 0, Positive (*P*) = 0.8, Positive Big (*PB*) = 1. The implemented T1-FLCs use the product implication and the weighted average defuzzification method.

1) Optimized Type-1 Fuzzy PID Controller

In design strategy of the Optimized T1-FPD (OT1-FPID) controller, the input and output SFs are selected as optimization variables while the antecedent and consequent MFs and rule base are fixed. We will employ an optimization procedure where the IAE performance measure is minimized via Big Bang – Big Crunch (BB-BC) algorithm [19] to optimize the SFs. The IAE is defined as

$$IAE = \int_{t=0}^{\infty} |e|\, dt \tag{2}$$

In the optimization procedure, we will only optimize the K_d, K_a, K_b while K_e is calculated as follows:

$$K_e = \frac{1}{r(t_f) - y(t_f)} \tag{3}$$

where $r(t_f)$ and $y(t_f)$ are the values of the reference and system output at the time of the reference variation (t=t_f) [5].

2) Function Tuner Based Type-1 Fuzzy PID Controller

The first employed self-tuning T1-FPID structure is the FTT1-FPID controller [8]. The structure of STT1-FPID is shown in Fig.2. Here, the self-tuning mechanism adjusts the SFs in an online manner as follows:

$$K_b = f(e)K_b^0 \tag{4}$$

$$K_d = g(e)K_d^0 \tag{5}$$

where K_b^0 and K_d^0 are the initial values of the integral and derivative SFs. Here, $f(e)$ and $g(e)$ represent nonlinear mappings as follows:

$$f(e) = a_1|e| + a_2 \quad (6)$$

$$g(e) = b_1|1 - e| + b_2 \quad (7)$$

where a_1, a_2, b_1 and b_2 are the tuning parameters to be determined. More detailed information about FTT1-FPID structure can be found in [8].

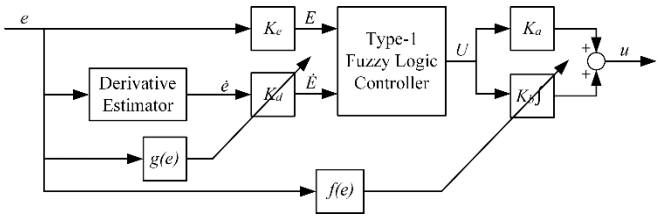

Fig. 2. FTT1-FPID controller structure

In the design of the FTT1-FPID controller, the same input and output MFS and rule base of the T1-FPID are employed. Moreover, we will set initial values of the SFs to the SFs of OT1-FPID controller (K_b^0=K_b, K_d^0=K_d). Even though the self-tuning mechanism provides extra degree of freedom to T1-FPID structure, it presents new tuning parameters to be determined. Thus, in the design of the FTT1-FPID, there will be four new tuning parameters (a_1, a_2, b_1 and b_2) optimized to minimize the IAE via BB-BC.

3) Function Relative Rate Observer Based Type-1 Fuzzy PID Controller

The second presented STT1-FPID controller structure is the RROT1-FPID controller [9]. In this self-tuning structure, the derivative and integral SFs are adjusted in online manner with respect to relative rate which gives information about the speed of the system response and is defined as [9]:

$$r_v = \frac{de(k) - de(k-1)}{de(.)} = \frac{dde(k)}{de(.)} \quad (8)$$

where $de(k)$ is the incremental change in error at discrete instant, $dde(k)$ is the incremental change in $de(k)$ and $de(.)$ defined as

$$de(.) = \begin{cases} de(k) & if\ |de(k)| \geq |de(k-1)| \\ de(k-1) & if\ |de(k)| < |de(k-1)| \end{cases} \quad (9)$$

The block diagram of RROT1-FPID controller is shown in Fig.3. Here, the integral and derivative SFs are adjusted as

$$K_b = K_b^0 / K_f \gamma \quad (10)$$

$$K_d = K_d^0 K_f K_{fd}\, \gamma \quad (11)$$

where K_b^0 and K_d^0 are the initial values of the SFs, Here, γ is the update coefficient and is generated from the fuzzy parameter regulator as shown in Fig.3. The fuzzy parameter regulator is a Mamdani type fuzzy system consists of a 3x4 rule base where the inputs are r_v and e and the antecedent consequent part is defined with T1-FSs. K_f is the output SF of the fuzzy parameter regulator and K_{fd} is an additional SF that affects only the derivative SF of the RROT1-FPID. Detailed information about RROT1-FPID structure and the parameter regulator is presented in [9].

In design strategy of RROT1-FPID controller, the input and output MFs, rule base, SFs are set to T1-FPID ones. Moreover, we will set initial values of the SFs (K_b^0 and K_d^0) equal to the SFs of T1-FPID controller (K_b^0=K_b, K_d^0=K_d). Even though the self-tuning mechanism provides extra degree of freedom to T1-FPID structure, it presents new tuning parameters and an extra fuzzy inference system. Thus, in the design procedure of the RROT1-FPID only K_f and K_{fd} gains will be optimized via BB-BC to minimize the IAE while the internal parameters (MFs, rule-base) of fuzzy parameter regulator are set to the values given in [9].

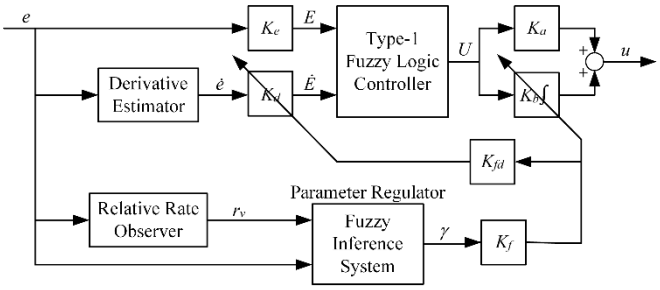

Fig. 3. RROT1-FPID controller structure

B. Design Strategy of the Interval Type-2 Fuzzy PID Controller

In this subsection, we will present the general structure of the employed IT2-FPID controller and then an optimization based design strategy.

In the design of the IT2-FPID, we will employ the same symmetrical 3x3 rule base and consequent MFs of T1-FPID. Thus, the rule structure of the IT2-FLC is as follows:

$$R_q\text{: IF } E \text{ is } \tilde{A}_{1j} \text{ and } E \text{ is } \tilde{A}_{2j} \text{ THEN } U \text{ is } C_q, \quad i,j = 1,2,3;\ \ q = 1,\dots,Q = 9 \quad (12)$$

where C_q is the consequent crisp set, Q is the number of rules and $\tilde{A}_{1j}$ and $\tilde{A}_{2j}$ are the antecedent IT2-FSs. We will denote the IT2-FSs as *N* (Negative), *Z* (Zero) and *P* (Positive). The antecedent IT2-FSs can be described in terms of upper MFs ($\overline{\mu}_{\tilde{A}_{1i}}$ and $\overline{\mu}_{\tilde{A}_{2i}}$) and lower MFs ($\underline{\mu}_{\tilde{A}_{1i}}$ and $\underline{\mu}_{\tilde{A}_{2i}}$) which creates the FOU (which provides extra degree of freedom) in IT2-FSs. The antecedent IT2-FSs are defined with four parameters (l_{ij}, c_{ij}, r_{ij}, m_{ij}; *i=1,2, j=1,2,3*), as shown in Fig.1d. In this study, we will set as l_{11}=l_{21}=-1, c_{11}=c_{21}=0, r_{11}=r_{21}=1 (the same values of the T1-FPID ones). Thus, the FOU will be created by the heights of the lower MFs (m_{ij}; *i=1,2, j=1,2,3*) of the IT2-FLC. The implemented IT2-FLC uses the center of sets type reduction/ defuzzification method [22].

In design strategy of the IT2-FPID, we will set the output MFs, rule base, SFs to the same values of T1-FPID ones. Thus, there are 6 parameters to be designed (m_{ij}; *i=1,2, j=1,2,3*). However, we employ m_{11}= m_{13} and m_{21}= m_{23} to have symmetrical antecedent MFs. Consequently, the design parameters of the IT2-FPID are m_{11}=m_{13}, m_{12}, m_{21}=m_{23} and m_{22}. We will employ a BB-BC based optimization procedure to tune the height of the lower antecedent MFs with respect to the IAE measure. Even though the FOU provides extra degree of freedom to IT2-FPID structure, it increases the number of parameters to be designed. However, it will be shown later shown in the real-time control applications that the Optimized IT2-FPID (OIT2-FPID) produces a superior control performances.

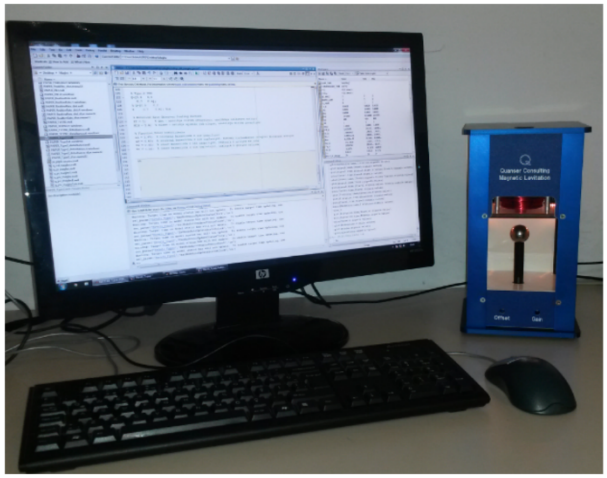

(a)

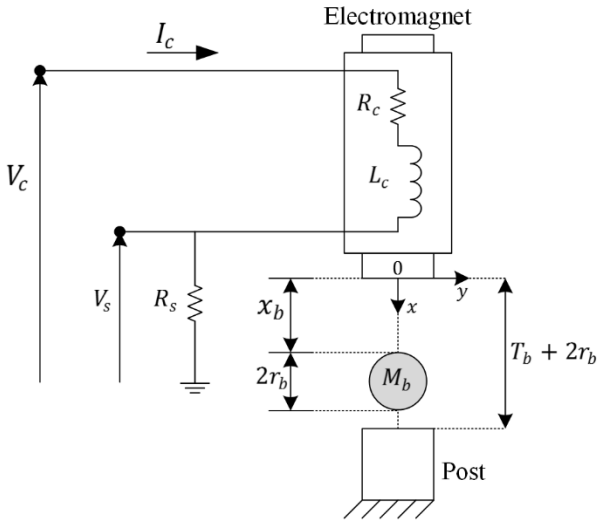

(b)

Fig. 4. (a) MAGLEV experimental setup, (b) Block diagram of MAGLEV

III. Control System Design Strategy for the MAGLEV

In this section, we will present brief information about the handled real-time QUANSER Magnetic Levitation Plant experimental setup, and then we will present the cascade control structure for the MAGLEV. Finally we will present the real-time experimental results.

A. MAGLEV System Description

In this subsection, we will present brief information about the employed QUANSER-MAGLEV which is shown in Fig.4a. The experimental setup consists of a single input which is the coil voltage (V_c), and two outputs which are the coil current (I_c) and ball position (x_b). The model of the MAGLEV systems consists of two parts which are the electrical and mechanical model. The differential equations related to the MAGLEV system are [23]:

$$\frac{\partial}{\partial t} I_c = \frac{V_c - (R_c + R_s) I_c}{L_c} \tag{13}$$

$$\frac{\partial^2}{\partial t^2} x_b = -\frac{K_m I_c^2}{2 M_b x_b^2} + g \tag{14}$$

where R_c is coil resistance, R_s is current sense resistance, L_c is coil inductance, K_m is electromagnet force constant, M_b is ball mass, g is gravitational constant. The corresponding schematic diagram is given in Fig.4b and the parameters are R_c=10Ω, R_s =1Ω, L_c=412.5mH, g =9.81m/s^2, K_m=6.53E-5N.m^2/A^2, M_b=0.068kg, r_b=1.27E-2m, T_b=0.014 m [23].

B. MAGLEV Cascade Control Structure

In this section, we will present the employed cascade control structure (shown in Fig.5) for the MAGLEV. In this structure, we will employ a PI controller in the inner loop which is as given

$$V_c = K_{pc} e_c + K_{ic} \int e_c dt \tag{15}$$

where e_c (e_c=I_d-I_c) is error between desired coil current (I_d) and measured coil current (I_c), K_{pc} and K_{ic} are PI gains of the inner loop controller. The inner PI controller is designed via pole placement design procedure and the PI parameters are found as K_{pc}=182.875, K_{ic} =24801. Throughout this study, we keep the inner PI controller fixed.

We will employ the presented T1-FPID, FTT1-FPID, RROT1-FPID and IT2-FPID structures as the outer loop controllers. The implemented T1-FPID and IT2-FPID controllers' parameters are determined by using optimization procedure based design strategies that are presented in Section II. Moreover, we will compare the results of the FPID controllers with a conventional PID controller which is defined as:

$$I_d = K_{px} e_x + K_{ix} \int e_x dt + K_{dx} \frac{de_x}{dt} \tag{16}$$

where e_x (e_x= x_d-x_b) is error between desired ball position (x_d) and measured ball position (x_b) and K_{px}, K_{ix}, K_{dx} are the controller parameters of outer loop PID controller. The PID controller parameters are also optimized with respect to the IAE performance measure via BBBC. During the optimization procedures of the FPID and PID structures, the population size and iteration number of BB-BC are set to 20 and 100 respectively.

The employed controllers are optimized with respect to a varying reference trajectory with the values of 11, 9 and 11mm (training reference trajectory). It will be assumed that the MAGLEV is at steady state point at x_b^0=12mm, I_c^0=1.72A and V_c^0=18.87V. For the training reference trajectory, the parameters of the Optimized PID (OPID) and OT1-FPID are obtained as K_{px}=227.03, K_{ix}=492.39, K_{dx}=4.2 and K_d=11.2 K_a =0.67 K_b =2.21. Note that K_e will be calculated via Equation (3) with respect to the reference signal. The parameters of the FTT1-FPID controller are found as a_1=1.67, a_2=0.53, b_1=0.01 and b_2=1.07 while the optimized parameters of the RROT1-FPID are K_f =1.74 and K_{fd}=1.23. The design parameters of OIT2-FPID controller are found as m_{11}=m_{13}=0.81, m_{12}=0.32, m_{21}=m_{23}=0.70, m_{22}=0.59.

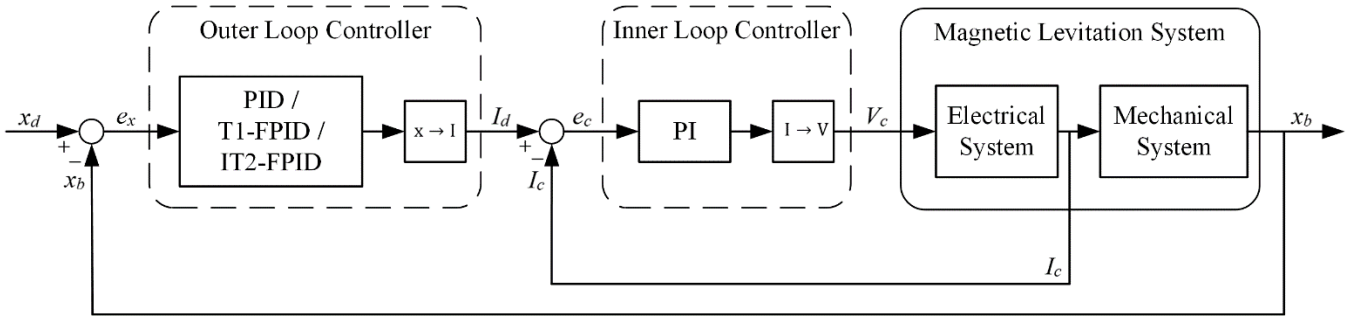

Fig. 5. Cascade control structure

C. Real-Time Experimental Results

In this subsection, we will present two analyses in order to compare the control performances of the OPID, OT1-FPID, FTT1-FPID, RROT1-FPID and IT2-FPID cascade control structures with respect to the Settling Time (T_s), Overshoot (OS%) and the IAE performance measures. At first we will analyze and present the control performances for the training reference trajectory in presence of measurement noise. Then, the ability of controllers to handle unknown system dynamics and noise will be investigated by defining a testing reference trajectory at which the controllers are not optimized.

In order to clearly show the superiority of the OIT2-FPID, we will present the real-time control results in two groups with respect to their structures. Thus, we will present and compare the OIT2-FPID structure with the non-self-tuning controller structures OPID and OT1-FPID; and then with the self-tuning structures FTT1-FPID and RROT1-FPID (which provide extra degrees of freedom to the T1-FPID structure) to have an easier analysis.

1) Control Performances for the Training Reference Trajectory

We will first examine the control performances of the controllers for the training reference trajectory with the values of 11, 9 and 11 mm (at which they are optimized). The comparison between OIT2-FPID and the non-self-tuning structures is given in Fig.6a while the comparison between OIT2-FPID and the self-tuning structures and Fig.6b. The obtained performance measures are tabulated in Table I.

In order to examine the transient state performances (Ts, OS %) of the control systems, we will examine the reference value variation from 11 mm to 9 mm in detail. In comparison with the OPID and OT1-FPID structures, the OIT2-FPID structure reduced settling time to 0.71 s and the overshoot to 11%. Moreover, if we examine the performances of the RROT1-FPID and FTT1-FPI, it can be concluded that the employed self-tuning mechanisms were able to enhance the T1-FPID control system performance. However, in comparison with RROT1-FPID, OIT2-FPID has reduced the overshoot by about 45% while it has increased the settling time relatively (which is still satisfactory). Whereas in the comparison with FTT1-FPID, the OIT2-FPID decreased the settling time about 23% while the overshoot value is almost the same. Moreover, as it can be clearly seen in Table I, the OIT2-FPID structure has an overall better IAE performance measure in comparison to the other employed controllers.

It can be concluded that the OIT2-FPID structure was able to enhance the control system performance of the MAGLEV in comparison to both non-self-tuning (OPID and OT1-FPID) and self-tuning structures (FTT1-FPID and RROT1-FPID). Moreover, although the self-tuning mechanisms provide the T1-FPID controller structures with extra degrees of freedom, their performance results were not good as the OIT2-FPID ones in presence of noise since the their tuning mechanism is based on the value of the error. Thus, it can be concluded that the FOU of the OIT2-FPID give the opportunity to type-2 fuzzy structure to enhance the control performance and provides robustness against noise.

2) Control Performances for the Testing Reference Trajectory

In this subsection, we will examine the control performances of the controllers for a reference trajectory at which they are not optimized in order to examine their robustness against unknown dynamics. Thus, we will employ a varying testing reference trajectory with the values 12 mm, 11 mm and 9 mm where the MAGLEV is initially at the steady state point x_b^0=11mm, I_c^0=1.57A and V_c^0=17.29V. The comparison between OIT2-FPID and the non-self-tuning controller structures is given in Fig.7a, while the comparison between OIT2-FPID and the self-tuning controller structures is given in Fig.7b. As it can be clearly seen in the Table I, OIT2-FPID structure has better control performance in comparison to the other controllers.

For instance, for the reference value variation from 10mm to 9mm, OPID control system has worst performance measures. Here, both employed STT1-FPID structures enhanced the OT1-FPID structure but the FTT1-FPID structure has best IAE performance measure. In comparison with the OT1-FPID structure, the FTT1-FPID reduced settling time by about 27% while the OIT2-FPID structure reduced settling time by about 48% while both the FTT1-FPID and OIT2-FPID structures reduced the overshoot by about 67%. Moreover, for the reference variation form 11 mm to 12 mm, the OPID and OT1-FPID controller structures have an oscillating system response, while the OIT2-FPID and FTT1-FPID and RROT1-FPID structures ended up with stable system responses where the OIT2-FPID has the fastest system response.

It can be concluded that, the controller structures that have extra degrees of freedom (OIT2-FPID, FTT1-FPID and RROT1-FPID) have better transient responses and overall performance. Moreover, the extra degree of freedom (FOU)

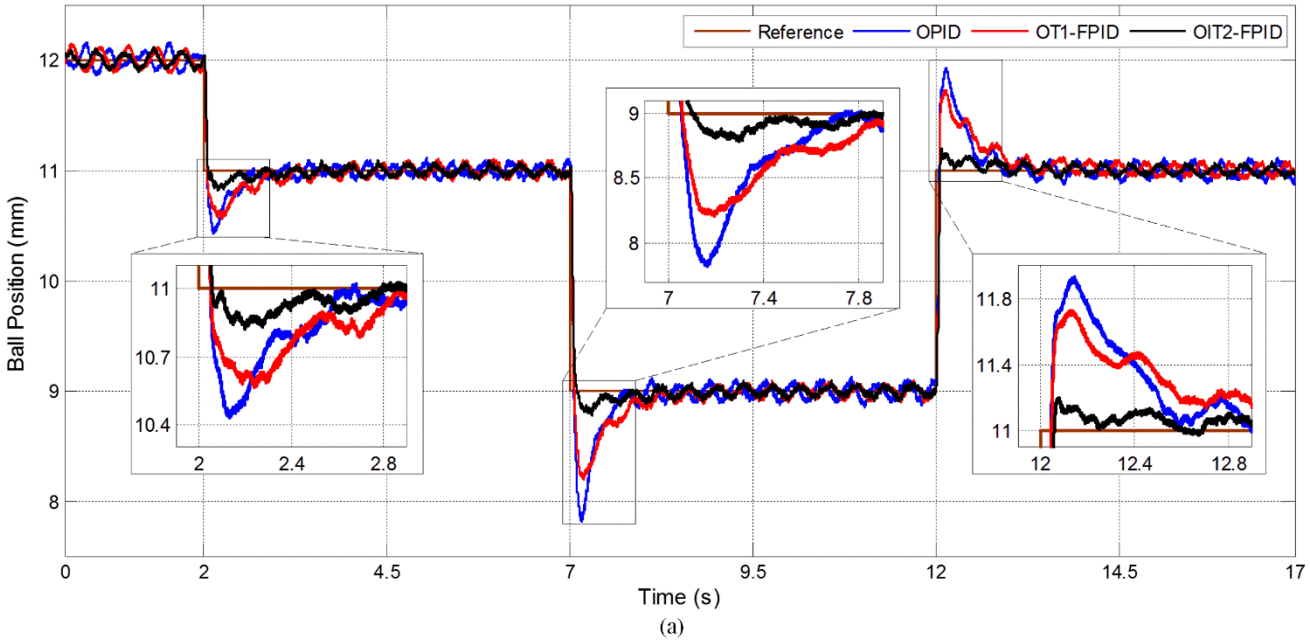

(a)

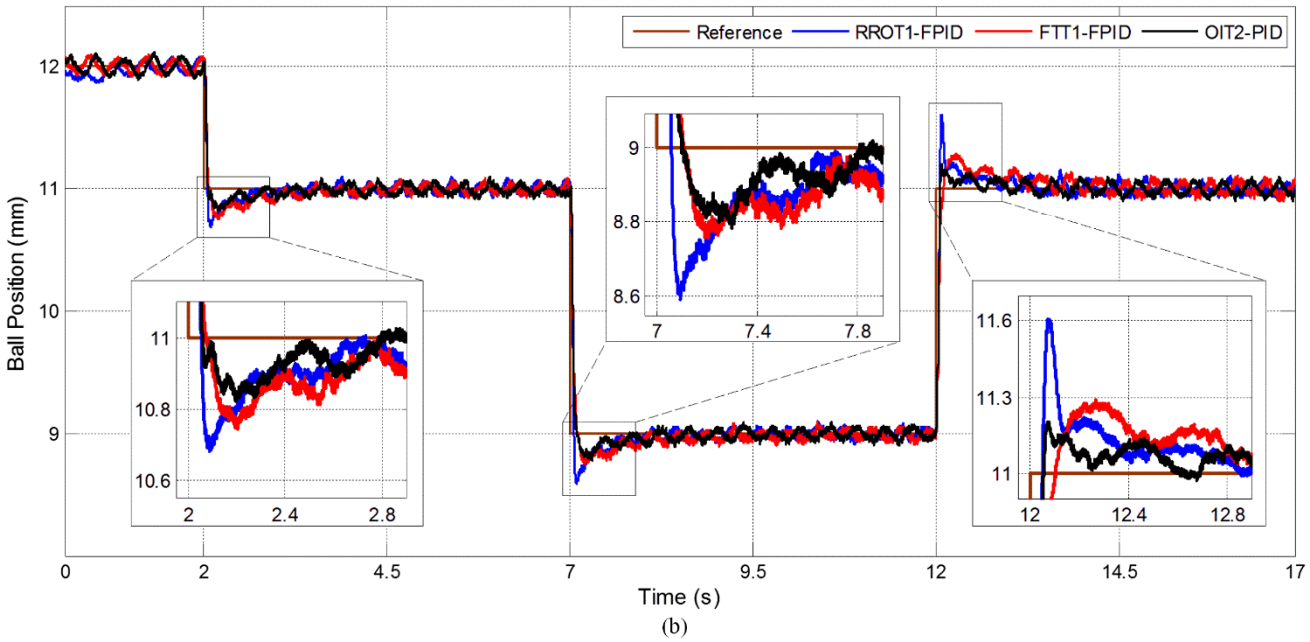

(b)

Fig. 6. Experimental results for the training reference trajectory

of the IT2-FSs provides the OIT2-FPID structure to have satisfactory control performances when compared to self-tuning structures. Consequently, the OIT2-FPID controller structure provided comparatively good control performances in presence of noise and unknown dynamics compared to both non-self-tuning and self-tuning structures.

D. Computational Times of Implemented Controllers

In this subsection, we have investigated the computation time needed by the IT2-FPID and T1-FPID structures to establish if their more complex structures will cause drastic impact on the controller real-time response. Thus, we have calculated the times needed by the type-1 and type-2 fuzzy controllers to map an input to an output for all possible combinations of the input values in their corresponding universe of discourses, i.e., $e \in [-1,+1]$ and $\dot{e} \in [-1,+1]$. This procedure has been repeated 100 times and the average computational times are calculated by the mean values of entire test results. The calculations are done on a personal computer with following specifications; Intel Core i7–3630Q 2.48GHz CPU and 16 GB RAM.

The calculated average computational time of T1-FLC is 0.0147 s, while the average computational time of IT2-FLC is 0.076 s. The average computational time of FTT1-FPID is calculated 0.015 s, while the average time of RROT1-FPID is calculated 0.0297 s. STT1-FPID structures need extra time when compared to their type-1.

Although there is some increase in the average computation time of the IT2-FPID in comparison to the T1-FPID structures, the real-time control application of the

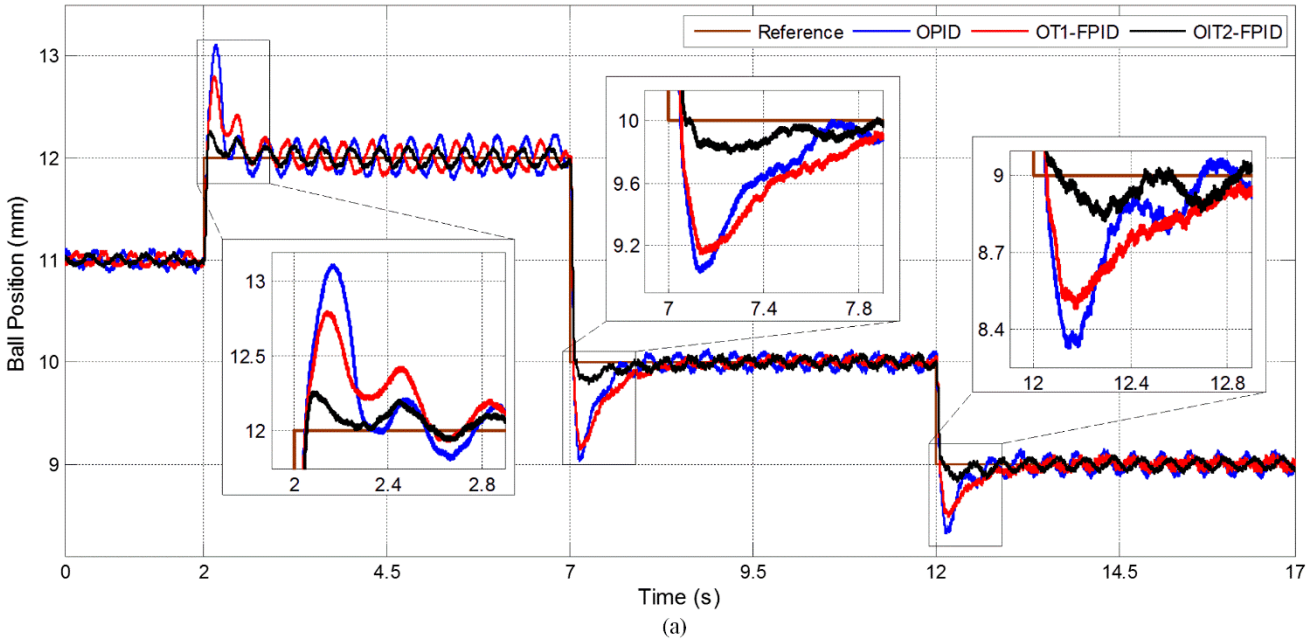

(a)

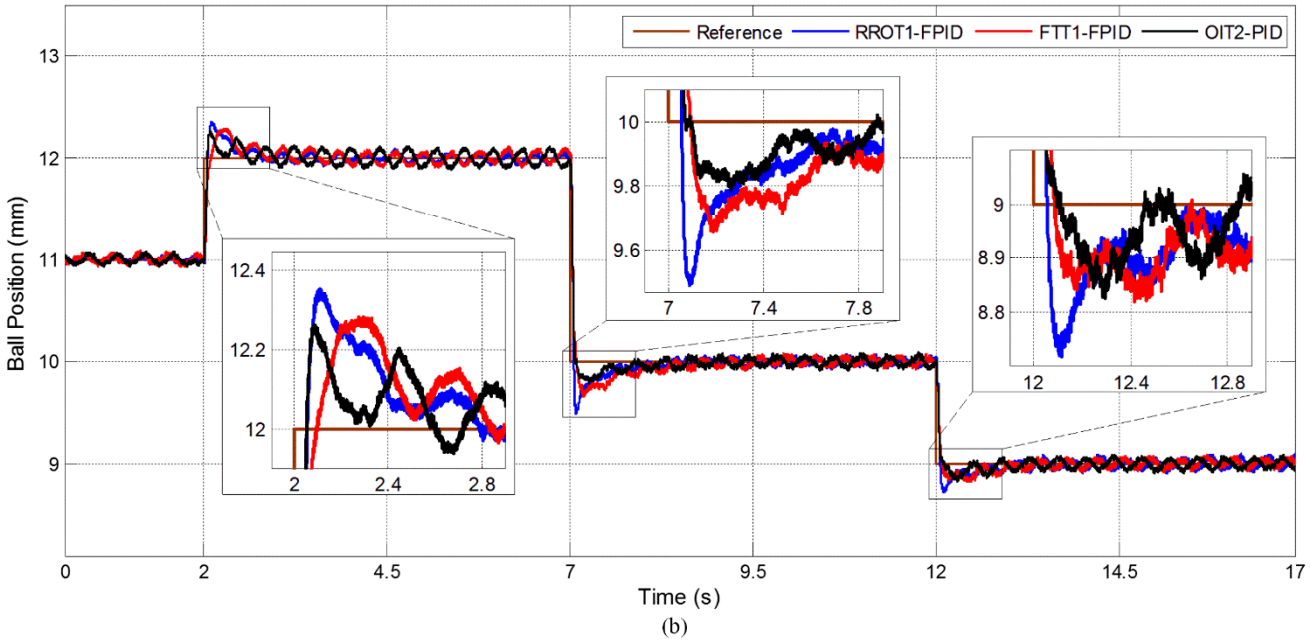

(b)

Fig. 7. Experimental results for the testing reference trajectory

IT2-FPID is still feasible for systems with relatively small sampling periods and as it has been shown the OIT2-FPID produces superior control performances in comparison to its type-1 and self-tuning type-1 counterparts.

IV. Conclusions

In this paper, we presented comparative real-time results between T1-FPID, IT2-FPID controller structures on the real time MAGLEV experimental setup. As part of this study, we also considered a STT1-FPID structure which has more extra degree freedoms since the fuzzy rule weights are handled as online tuning parameters. Thus, we also analyzed the control performances of the RROT1-FPID and FTT1-FPID in comparison with the OIT2-FPID structure. Since, the employed self-tuning mechanisms allow the T1-FPID structures to have more degrees of freedom; we investigated if the power of the IT2-FPID lies in its ability to handle the high level of uncertainties rather than only having an extra degree of freedom. We implemented the presented FPID controllers in a cascade structure to solve the control problem of the MAGLEV.

A detailed comparative study has been conducted to show that the real-time control performance of the IT2-FPID is better in different operating points even at those at which the controllers are not optimized and IT2-FPID control system is more robust against noise and unknown system dynamics when compared to its T1-FPID, STT1-FPID and traditional PID counterparts.

TABLE 1. EXPERIMENTAL RESULTS

	THE TRAINING REFERENCE TRAJECTORY							THE TESTING REFERENCE TRAJECTORY						
	TRANSIENT PERFORMANCE							TRANSIENT PERFORMANCE						
	12-11 mm		11-9 mm		9-11 mm			11-12 mm		12-10 mm		10-9 mm		
	Ts	OS	Ts	OS	Ts	OS	IAE	Ts	OS	Ts	OS	Ts	OS	IAE
OPID	0.57 s	57%	0.98 s	59%	0.85 s	47%	1.532	*	*	0.92 s	48%	0.99 s	67%	1.798
OT1-FPID	0.79 s	44%	1.12 s	40%	1.23 s	36%	1.518	*	*	1.12 s	43%	0.76 s	52%	1.530
FTT1-FPID	0.63 s	25%	0.92 s	12%	0.79 s	14%	0.979	1.44 s	28%	1.29 s	17%	0.55 s	18%	0.842
RROT1-FPID	0.45 s	32%	0.61 s	20%	0.66 s	30%	0.874	0.39 s	35%	0.89 s	25%	0.57 s	28%	0.932
OIT2-FPID	0.36 s	18%	0.71 s	11%	0.48 s	10%	0.779	0.54 s	26%	0.77 s	11%	0.39 s	17%	0.875

* oscillating system response

The outcomes of the comparative studies showed that the reason for the superior control performance of IT2-FPID in comparison to STT1-FPID structures (which have extra degrees of freedom related to the self-tuning SFs) under high levels of uncertainty and noise is not merely for its use of extra parameters, but rather its different way of dealing with the uncertainties and noise present in real world.

REFERENCES

[1] S. Galichet and L. Foulloy, "Fuzzy controllers: synthesis and equivalences," *IEEE Transactions on Fuzzy Systems*, vol. 3 (2), pp. 140–148, 1995.

[2] T. T. Huang, H. Y. Chung and J. J. Lin, "A fuzzy PID controller being like parameter varying PID," *IEEE International Fuzzy Systems Conference Proceeding*, vol. 1, pp. 269–275, 1999.

[3] W. Z. Qiao and M. Mizumoto, "PID type fuzzy controller and parameters adaptive method," *Fuzzy Sets and Systems*, vol. 78, (1), pp. 23–35, 1996.

[4] H. X. Li and H. B. Gatland, "Conventional fuzzy control and its enhancement," *IEEE Transactions on Systems, Man and Cybernetics Part B*, vol. 26 (5), pp. 791–797, 1996.

[5] X. G. Duan, H. X. Li and H. Deng, "Effective tuning method for fuzzy PID with internal model control," *Industrial & Engineering Chemistry Research*, vol. 47, pp. 8317–8323, 2008.

[6] B. Hu, G. K. I. Mann and R. G. Gasine, "New methodology for analytical and optimal design of fuzzy PID controllers," *IEEE Transactions on Fuzzy Systems*, vol. 7 (5), pp. 521–539, 1999.

[7] R. K. Mudi and N. R. Pal, "A robust self-tuning scheme for PI- and PD-type fuzzy controllers," *IEEE Transactions on Fuzzy Systems*, vol. 7 (1), pp. 2–16, 1999.

[8] Z. W. Woo, H. Y. Chung and J. J. Lin, "A PID-type fuzzy controller with self-tuning scaling factors," *Fuzzy Sets Systems*, vol. 115, pp. 321–326, 2000.

[9] M. Guzelkaya, I. Eksin and E. Yesil, "Self-tuning of PID-type fuzzy logic controller coefficients via relative rate observer," *Engineering Applications of Artificial Intelligence*, vol. 16, pp. 227–236, 2003.

[10] K. K. Ahn and D. Q. Truong, "Online tuning fuzzy PID controller using robust extended Kalman filter," *Journal of Process Control*, vol. 19, pp. 1011–1023, 2009.

[11] O. Karasakal, M. Guzelkaya, I. Eksin and E. Yesil, "An error-based on-line rule weight adjustment method for fuzzy PID controllers," *Expert Systems and Applications*, vol. 38 (8), pp. 10124–10132, 2011.

[12] O. Karasakal, M. Guzelkaya, I. Eksin, E. Yesil and T. Kumbasar, "Online tuning of fuzzy PID controllers via rule weighting based on normalized acceleration," *Engineering Applications of Artificial Intelligence*, vol. 26 (1), pp. 184–197, 2013.

[13] D. Wu and W. W. Tan, "Interval Type-2 Fuzzy PI Controllers: Why They Are More Robust," *IEEE International Conference on Granular Computing*, pp. 802–807, 2010.

[14] D. Wu, "On the Fundamental Differences between Type-1 and Interval Type-2 Fuzzy Logic Controllers," *Transactions on Fuzzy Systems*, vol. 20, no. 5, pp. 832–848, 2012.

[15] H. Hagras, "A Hierarchical Type-2 Fuzzy Logic Control Architecture for Autonomous Mobile Robots," *IEEE Transactions on Fuzzy Systems*, vol. 12 (4) pp. 524–539, 2004.

[16] O. Castillo and P. Melin, *Type-2 Fuzzy Logic Theory and Applications*. Berlin, Germany: Springer-Verlag, 2008.

[17] D. Wu and W. W. Tan, "A simplified type-2 fuzzy logic controller for real-time control," *ISA Transactions*, vol. 45 (4), pp. 503–516, 2006.

[18] T. Kumbasar, I. Eksin, M. Guzelkaya and E. Yesil, "Type-2 fuzzy model based controller design for neutralization processes," *ISA Transactions*, vol. 51 (2), pp. 277–287, 2012.

[19] T. Kumbasar and H. Hagras, "A Big Bang-Big Crunch optimization based approach for interval type-2 fuzzy PID controller design," *IEEE International Conference on Fuzzy Systems*, pp. 1-8, 2013.

[20] T. Kumbasar, "A simple design method for interval type-2 fuzzy PID controllers", *Soft Computing*, 2013. (article in press)

[21] E. Yesil, "Interval type-2 fuzzy PID load frequency controller using Big Bang-Big Crunch optimization," *Applied Soft Computing*, vol. 15, pp. 100-112, 2014.

[22] Q. Liang and J. M. Mendel, "Interval type-2 fuzzy logic systems: theory and design," *IEEE Transactions on Fuzzy Systems*, vol. 8 (5), pp. 535–550, 2000.

[23] QUANSER MAGLEV user manual.